



Microstructure and interfacial properties of $\text{HfO}_2\text{-Al}_2\text{O}_3$ nanolaminate films

M. Liu^{a,*}, G. He^a, L.Q. Zhu^a, Q. Fang^{a,b}, G.H. Li^a, L.D. Zhang^a

^a Key Laboratory of Materials Physics, Institute of Solid State Physics, China Academy of Sciences,
P.O. Box 1129, Hefei 230031, PR China

^b Electronic and Electrical Engineering, University College London, Torrington Place, London WC1E 7JE, UK

Received 20 April 2005; received in revised form 10 August 2005; accepted 13 August 2005

Available online 12 September 2005

Abstract

High- k $\text{HfO}_2\text{-Al}_2\text{O}_3$ composite gate dielectric thin films on Si(1 0 0) have been deposited by means of magnetron sputtering. The microstructure and interfacial characteristics of the $\text{HfO}_2\text{-Al}_2\text{O}_3$ films have been investigated by using X-ray diffraction (XRD), Fourier transform infrared spectroscopy (FTIR) and spectroscopic ellipsometry (SE). Analysis by XRD has confirmed that an amorphous structure of the $\text{HfO}_2\text{-Al}_2\text{O}_3$ composite films is maintained up to an annealing temperature of 800 °C, which is much higher than that of pure HfO_2 thin films. FTIR characterization indicates that the growth of the interfacial SiO_2 layer is effectively suppressed when the annealing temperature is as low as 800 °C, which is also confirmed by spectroscopy ellipsometry measurement. These results clearly show that the crystallization temperature of the nanolaminate $\text{HfO}_2\text{-Al}_2\text{O}_3$ composite films has been increased compared to pure HfO_2 films. Al_2O_3 as a passivation barrier for HfO_2 high- k dielectrics prevents oxygen diffusion and the interfacial layer growth effectively.

© 2005 Elsevier B.V. All rights reserved.

PACS: 77.55.+f; 78.20.Ci; 81.15.Cd

Keywords: Interface; Magnetron sputtering; Crystallization

1. Introduction

A practical limitation of using SiO_2 as the gate dielectric of metal-oxide-semiconductor (MOS) tran-

sistor is about 1.5 nm in thickness due to direct tunneling of electrons through such thin SiO_2 . However, in order to achieve the required higher speed and lower power of an ultra-large scale integration device in the near future, the thickness of a SiO_2 gate dielectric film will have to be as thin as about 1 nm. Therefore, to prevent the increase of the leakage current while maintaining the same gate

* Corresponding author. Tel.: +86 551 5591465 424;

fax: +86 551 5591434.

E-mail address: mliu@issp.ac.cn (M. Liu).

capacitance equivalent to a thinner (~ 1.0 nm and below) SiO_2 layer, new gate dielectric materials with a significantly higher dielectric constant (high- k) are urgently required for microelectronic industry [1,2]. HfO_2 has emerged as one of the most promising high- k candidates due to its relatively high dielectric constant (~ 25), large band gap (~ 5.8 eV) and observed physical stability and calculated thermodynamic stability against silicon [3,4]. However, the physical and electrical properties of HfO_2 may suffer from its crystallization at high temperature during post-deposition annealing, which in turn induces higher leakage current and severe boron penetration issues [5]. More crucially, HfO_2 is a solid-state electrolyte for oxygen at high temperature [6]. High temperature annealing will lead to fast diffusion of oxygen through the HfO_2 , resulting in the growth of uncontrolled low- k interfacial layers. The uncontrolled low- k layers pose a serious limitation to further scaling of the equivalent oxide thickness (EOT) for HfO_2 gate dielectrics [7]. On the other hand, Al_2O_3 films synthesized directly on Si have been reported to remain amorphous up to 1000°C [8]. Some studies have focused on silicate and oxide alloys in an attempt to overcome the poor thermal stability. Especially, the nanolaminate structure composed of two high dielectric oxides represents a promising solution for enhancing thermal stability to sustain high dielectric and preventing oxygen diffusion [6,9]. Among the nanolaminates, $\text{HfO}_2\text{-Al}_2\text{O}_3$ shows a good thermal stability and higher dielectric constant at the high annealing temperature in the common process used in semiconductor industry [9].

Many techniques have been pursued to deposit $\text{HfO}_2\text{-Al}_2\text{O}_3$ composite thin films such as pulsed laser deposition, jet vapor deposition, and atomic layer deposition [9,10,12]. But to our knowledge, the characteristics of $\text{HfO}_2\text{-Al}_2\text{O}_3$ composite films fabricated by physical vapor deposition (PVD) have not been reported. In this work, rf magnetron sputtering and reactive sputtering techniques are utilized to synthesize nanolaminate $\text{HfO}_2\text{-Al}_2\text{O}_3$ composite films on Si(1 0 0). The microstructure, interfacial and optical properties of the films are systematically investigated in an annealing temperature ranging from 500 to 1000°C . The aim of this work is to study the crystallization temperature of the $\text{HfO}_2\text{-Al}_2\text{O}_3$ composite films and growth of the interfacial layer

between the composite film and silicon substrate at various annealing temperatures. Furthermore, a mechanism of the resistance to the oxygen diffusion in HfO_2 films due to the incorporation of Al_2O_3 layer, based on our experimental data, has also been discussed.

2. Experimental details

2.1. Preparation of $\text{HfO}_2\text{-Al}_2\text{O}_3$ films

The n-type Si(1 0 0) substrates with a resistivity of $2\text{--}5\ \Omega\ \text{cm}$ were pre-cleaned by a standard RCA cleaning, then the wafers were immersed in diluted HF (1%) solution for 10 s to remove native oxide and to hydrogen passivate the surface. After the chemical treatment process, the substrates were dried and directly put into the deposition chamber with a cylindrical stainless-steel chamber connected to a turbomolecular pump. The base pressure of the sputtering chamber before deposition was evacuated to 3.5×10^{-4} Pa and the working pressure during deposition was kept at 0.2 Pa. A nanolaminate $\text{HfO}_2\text{-Al}_2\text{O}_3$ composite film was deposited by three steps. Firstly, HfO_2 layer was pre-deposited on Si by rf magnetron sputtering with an Ar flow rate of 30 sccm. Secondly, Al_2O_3 layer was deposited by dc reactive sputtering with Ar/ O_2 mixture under flow rate of 30 and 10 sccm, respectively. Finally, the as-deposited film was in situ heated through the thermocouple. The deposition powers of HfO_2 and Al_2O_3 were kept at 100 and 56 W, respectively. The deposition rates of HfO_2 and Al_2O_3 films were kept at 0.2 and $0.1\ \text{\AA}/\text{s}$, respectively. The thickness of the HfO_2 and Al_2O_3 was 12 and 3 nm, respectively. In order to improve the qualities of the as-deposited $\text{HfO}_2\text{-Al}_2\text{O}_3$ films, the post-deposition annealing was performed in a furnace at different temperatures ranging from 500 to 1000°C for 20 min in Ar ambient.

2.2. Film characterization

The crystal structures of the films were examined by X-ray diffraction (XRD) using $\text{Cu K}\alpha$ radiation at 40 kV and 40 mA. Analysis of the interfacial layer formed between the $\text{HfO}_2\text{-Al}_2\text{O}_3$ nanolaminate films and the Si substrate was carried out on as-deposited

and annealed samples by Fourier transform infrared spectroscopy (FTIR) in a Nicolet Magna 750 operating in transmission mode. An ex situ phase modulated spectroscopic ellipsometry (UVISEL Jobin-Yvon) was used to measure the thickness and optical functions of the as-deposited and annealed $\text{HfO}_2\text{-Al}_2\text{O}_3$ nanolaminate films at room temperature in the spectral range 0.75–6.5 eV with a step of 50 meV at an incident angle of 70° .

3. Results and discussion

Fig. 1 shows XRD patterns of the as-deposited and annealed $\text{HfO}_2\text{-Al}_2\text{O}_3$ films at various temperatures. No diffraction peaks can be observed for the as-deposited film, indicating that the as-deposited $\text{HfO}_2\text{-Al}_2\text{O}_3$ film is an amorphous structure. The amorphous structure of the film can remain at an annealing temperature up to 800°C . When annealing temperature increases to 900°C , some relatively broad and weak multiple diffraction peaks emerge, which can be attributed to the monoclinic $\text{HfO}_2(-1\ 1\ 1)$, $(1\ 1\ 1)$ and $(2\ 0\ 0)$ planes. The large width and low intensity of the diffraction peaks suggest that very small grains are locally embedded in the amorphous structure. When the annealing temperature approaches 1000°C , some main peaks become sharp and more intense, implying an increase of the volume fraction of the crystalline phase in the $\text{HfO}_2\text{-Al}_2\text{O}_3$ films. From the position of the main peaks, it can be inferred that the crystalline

phase is monoclinic HfO_2 , not tetragonal HfO_2 . However, in our previous paper, a crystal phase contributed to tetragonal HfO_2 was observed in a pure HfO_2 film after annealing at 500°C [11]. It indicates that the crystallization of the $\text{HfO}_2\text{-Al}_2\text{O}_3$ nanolaminate composite structure during annealing is effectively suppressed. As we know, Al_2O_3 can remain amorphous when annealing temperature is higher than 1000°C ; thus, if incorporated with HfO_2 , the amorphous structure can be stabilized during high temperature annealing. Yu et al. have reported the $(\text{HfO}_2)_{0.67}(\text{Al}_2\text{O}_3)_{0.33}$ remained amorphous after 900°C annealing [12]. Cho et al. have identified that the structural transition from amorphous to crystalline for the $\text{Al}_2\text{O}_3\text{-HfO}_2$ nanolaminates occurs at a temperature of more than 900°C [13]. These results indicate that incorporating Al_2O_3 to HfO_2 matrix affects the nucleation and growth of HfO_2 grains from the composite matrix, so mixing of Al_2O_3 with HfO_2 will raise the crystallization onset temperature.

Currently, replacing SiO_2 with single high- k material layer, such as HfO_2 , ZrO_2 , Ta_2O_5 and Pr_2O_3 , is a main solution pursued by many groups. Unfortunately, it has been found that the formation of an interfacial layer between the grown dielectric layer and the silicon substrates always occurs due to the oxidation of the Si surface [14]. The amorphous SiO_2 layer on Si leaves dangling bonds that may result in electronic defects disrupting translation symmetry at the interface. It is desirable to minimize the thickness of any low- k SiO_2 layer between the high- k thin films and the Si substrate. FTIR analysis of the as-deposited and annealed samples is used in our work to monitor the interfacial layer formation (shown in Fig. 2). The infrared absorption spectra were obtained with the backside of all wafers etched in diluted HF to remove any native oxide and to subtract the absorbance of the sample and a reference sample from the same wafer without $\text{HfO}_2\text{-Al}_2\text{O}_3$ films. For the as-deposited film, as shown in Fig. 2(a), there is an absorption peak centered at 1107 cm^{-1} . According to the report from Alers et al. [15], for the Si wafers as substrates, a strong absorption centered at 1105 cm^{-1} attributed to the interstitial oxygen in the Si bulk. When the annealing temperature increases, it can be easy to see that the intensity of the absorption peak near 1107 cm^{-1} weakens (see Fig. 2(b)). Annealed at 900°C , a new broad absorption peak centered near

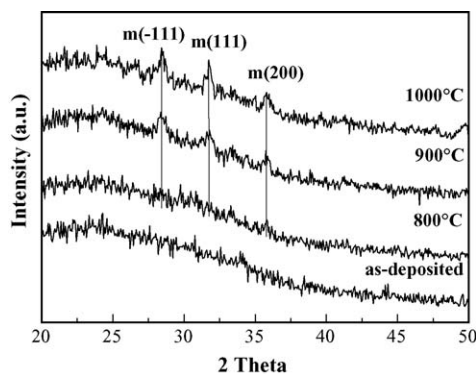


Fig. 1. XRD spectra of the as-deposited and post-deposition annealed samples at different temperatures. The letter 'm' represents the monoclinic structure of the HfO_2 film.

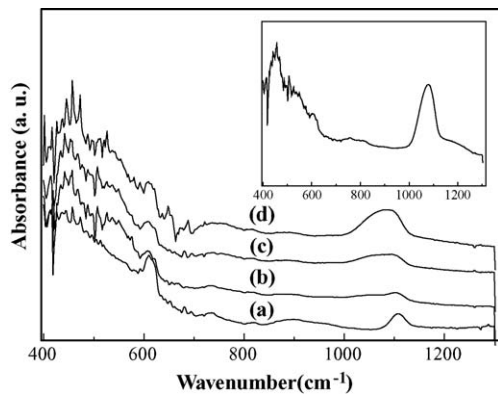


Fig. 2. FTIR absorbance spectra for the as-deposited and annealed samples at various temperatures: (a) as-deposited; (b) 800 °C; (c) 900 °C; (d) 1000 °C. The inset shows the FTIR spectrum of pure HfO₂ film on Si annealed at 1000 °C.

1070 cm⁻¹ appears (see Fig. 2(c)). This peak comes from the Si–O stretching mode [4], indicating the formation of interfacial SiO_x layer. In Fig. 2(d), the intensity of the absorption peak at 1070 cm⁻¹ increases at 1000 °C indicating that a thick SiO_x layer is formed between the deposited film and the Si(1 0 0) substrate.

Post-deposition annealing results in the release of the interstitial oxygen in the Si substrate; as a result, the peak intensity of 1107 cm⁻¹ decreases with the increase of annealing temperature before 800 °C. However, there is surface oxygen adsorbed in the film during the oxidation and deposition processes. When the post-annealing is carried out at low temperature, only a very small amount of these oxygen can penetrate the deposited layer into the Si substrate to form the SiO₂ interface, which can be seen in Fig. 2(c). For the high temperature annealing, the sample has already crystallized partly, shown in Fig. 1, which indicates that the oxygen diffusion along the grain boundaries of the high-*k* films becomes higher, inducing the uncontrollable growth of the interfacial SiO₂ layer between the Si and the HfO₂–Al₂O₃ films. Compared to pure HfO₂ film annealed at 1000 °C (inset in Fig. 2), however, the intensity of Si–O stretching peak at 1070 cm⁻¹ for pure HfO₂ is much higher than that for the nanolaminate HfO₂–Al₂O₃ composite films. It is well known that Al₂O₃ is a good oxygen diffusion barrier that may protect the Si surface from oxidation [16,17]. When incorporating

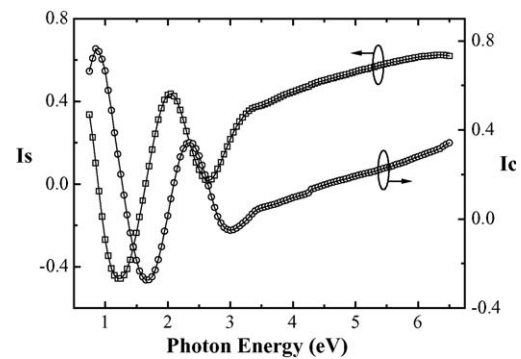


Fig. 3. Experimental (open circles) and fitted (solid lines) spectroscopic ellipsometric data for 500 °C annealed sample.

Al₂O₃ into HfO₂ layers, Al₂O₃ layer can effectively suppress oxygen diffusing and decrease the formation of low-*k* interfacial layer.

As a very useful and nondestructive technique, spectroscopic ellipsometry (SE) has been used to investigate the optical properties of HfO₂–Al₂O₃ thin films. A simple model of three-phase structure (substrate/HfO₂–Al₂O₃ film/HfO₂–Al₂O₃ film + void) has been established for the simultaneous fitting of measured parameters *I_s* and *I_c* of SE. Fig. 3 shows the experimental (open circles) and fitted (solid lines) spectra for the HfO₂–Al₂O₃ film annealed at 500 °C. Not shown here are the similar experimental data for the other samples annealed at different temperatures. It can be seen that for the as-deposited and low temperature annealed samples, a very good fit has been obtained without considering any interfacial layer. However, for the samples annealed in the range of 800–1000 °C, an interfacial SiO₂ layer has to be considered to obtain a reasonably good fit. Therefore, SE model should add a component of interfacial layer at higher temperatures. Fig. 4 shows the extrapolated refractive index spectra of the interfacial SiO₂ layers for 800 °C annealed sample together with those of pure SiO₂, the refractive index of the samples match very well at longer wavelengths. However, it is impossible to extract the correct values of refractive index of the interfacial layer by the fitting analysis of the SE data at shorter wavelengths, due to absorption by the HfO₂ layer. These SE results are in agreement with the FTIR measurements and further confirm the existence of the Si–O bonds between the HfO₂–Al₂O₃ films and Si substrates only when the films annealed at

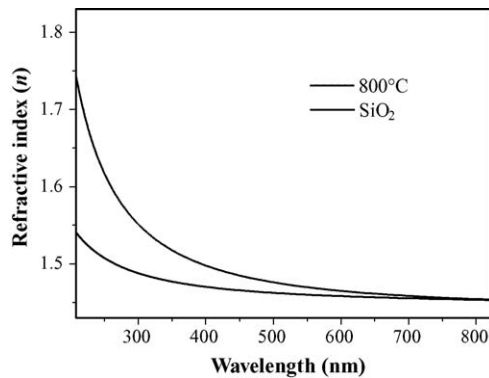


Fig. 4. The refractive index of the interfacial layers of 800 °C temperature annealed samples together with that of pure SiO₂.

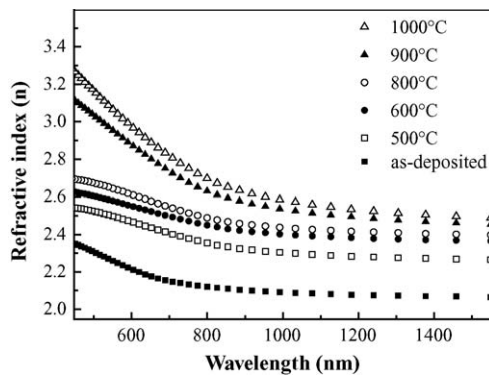


Fig. 5. Refractive indices calculated from the extracted best-fit parameters of a three-layer optical model for the HfO₂–Al₂O₃ films.

high temperatures. The refractive index n spectra of HfO₂–Al₂O₃ samples are shown in Fig. 5. The refractive index values of films increase with post-annealing temperature, which indicates that the density of the films increases with the annealing temperature. This increase of refractive index of the films with annealing temperature is attributed to the increase in packing density and crystallinity of the films at higher annealing temperatures, which is also conformed from the XRD analysis.

4. Conclusions

HfO₂–Al₂O₃ nanolaminate thin films have been deposited by magnetron sputtering techniques. The

structural, optical and interfacial properties of the as-deposited and annealed films have been investigated by XRD, FTIR and SE. XRD analysis shows that the films remain amorphous up to an annealing temperature of 800 °C, indicating that incorporating Al₂O₃ to HfO₂ increases the crystallization temperature. FTIR indicates that no interface layer forms during an annealing up to 800 °C. This result is in good agreement with the investigation through SE, which testifies that a very good fit has been obtained without considering any interfacial layer before 800 °C annealing. Optical constants of HfO₂–Al₂O₃ thin films have also showed that the density of the film increases with increase of annealing temperature.

Acknowledgement

We are grateful to National Major Project of Fundamental Research: Nanomaterials and Nanostructures.

References

- [1] A. Kurokawa, K. Nakamura, S. Ichimura, D.W. Moon, *Appl. Phys. Lett.* 76 (2000) 493.
- [2] H. Fukuda, M. Yasuda, T. Iwabuchi, *Appl. Phys. Lett.* 61 (1992) 693.
- [3] S.-G. Lim, S. Kriventsov, T. Jackson, J.H. Haeni, D.G. Schlom, A.M. Balbashov, R. Uecker, P. Reiche, J.L. Freeouf, G. Lucovsky, *J. Appl. Phys.* 91 (2002) 4500.
- [4] Q. Fang, J.-Y. Zhang, Z.M. Wang, M. Modreanu, B.J. O'Sullivan, P.K. Hurley, T.L. Leedham, D. Hywel, M.A. Audier, C. Jimenez, J.-P. Senateur, I.W. Boyd, *Thin Solid Films* 453–454 (2004) 203.
- [5] C.-L. Liu, Z.X. Jiang, R.I. Hegde, D.D. Sieloff, R.S. Rai, D.C. Gilmer, C.C. Hobbs, P.J. Tobin, S.F. Lu, *Appl. Phys. Lett.* 81 (2002) 1441.
- [6] G.D. Wilk, R.M. Wallace, J.M. Anthony, *J. Appl. Phys.* 87 (2000) 484.
- [7] G.D. Wilk, R.M. Wallace, J.M. Anthony, *J. Appl. Phys.* 89 (2001) 5243.
- [8] A. Chin, C.C. Liao, C.H. Lu, W.J. Chen, C. Tsai, *Symp. VLSI Tech. Dig.*, 1999, p. 135.
- [9] P.F. Lee, J.Y. Dai, K.H. Wong, H.L.W. Chan, C.L. Choy, *J. Appl. Phys.* 93 (2003) 3665.
- [10] W. Zhu, T.P. Ma, T. Tamagawa, Y. Di, J. Kim, R. Carruthers, M. Gibson, T. Furukawa, *Tech. Dig. Int. Electron Devices Meet.* 2001, p. 464.
- [11] G. He, Q. Fang, M. Liu, L.Q. Zhu, L.D. Zhang, *J. Cryst. Growth* 268 (2004) 155.

- [12] H.Y. Yu, N. Wu, M.F. Li, C. Zhu, B.J. Cho, D.-L. Kwong, C.H. Tung, J.S. Pan, J.W. Chai, W.D. Wang, D.Z. Chi, C.H. Ang, J.Z. Zheng, S. Ramanathan, *Appl. Phys. Lett.* 81 (2002) 3618.
- [13] M.-H. Cho, Y.S. Roh, C.N. Whang, K. Jeong, H.J. Choi, S.W. Nam, D.-H. Ko, J.H. Lee, N.I. Lee, F. Fujihara, *Appl. Phys. Lett.* 81 (2002) 1071.
- [14] B.-Y. Tsui, H.-W. Chang, *J. Appl. Phys.* 93 (2003) 10119.
- [15] G.B. Alers, D.J. Werder, Y. Chabal, H.C. Lu, E.P. Gusev, E. Garfunkel, T. Gustafsson, R.S. Urdahl, *Appl. Phys. Lett.* 73 (1998) 1517.
- [16] E.P. Gusev, M. Copel, E. Cartier, I.J.R. Baumvol, C. Krug, M.A. Gribelyuk, *Appl. Phys. Lett.* 76 (2000) 176.
- [17] M. Copel, E. Cartier, E.P. Gusev, S. Guha, N. Bojarczuk, M. Poppeller, *Appl. Phys. Lett.* 78 (2001) 2670.